Instabilities

Boundary Layer Meteorology

Laminar Boundary Layer

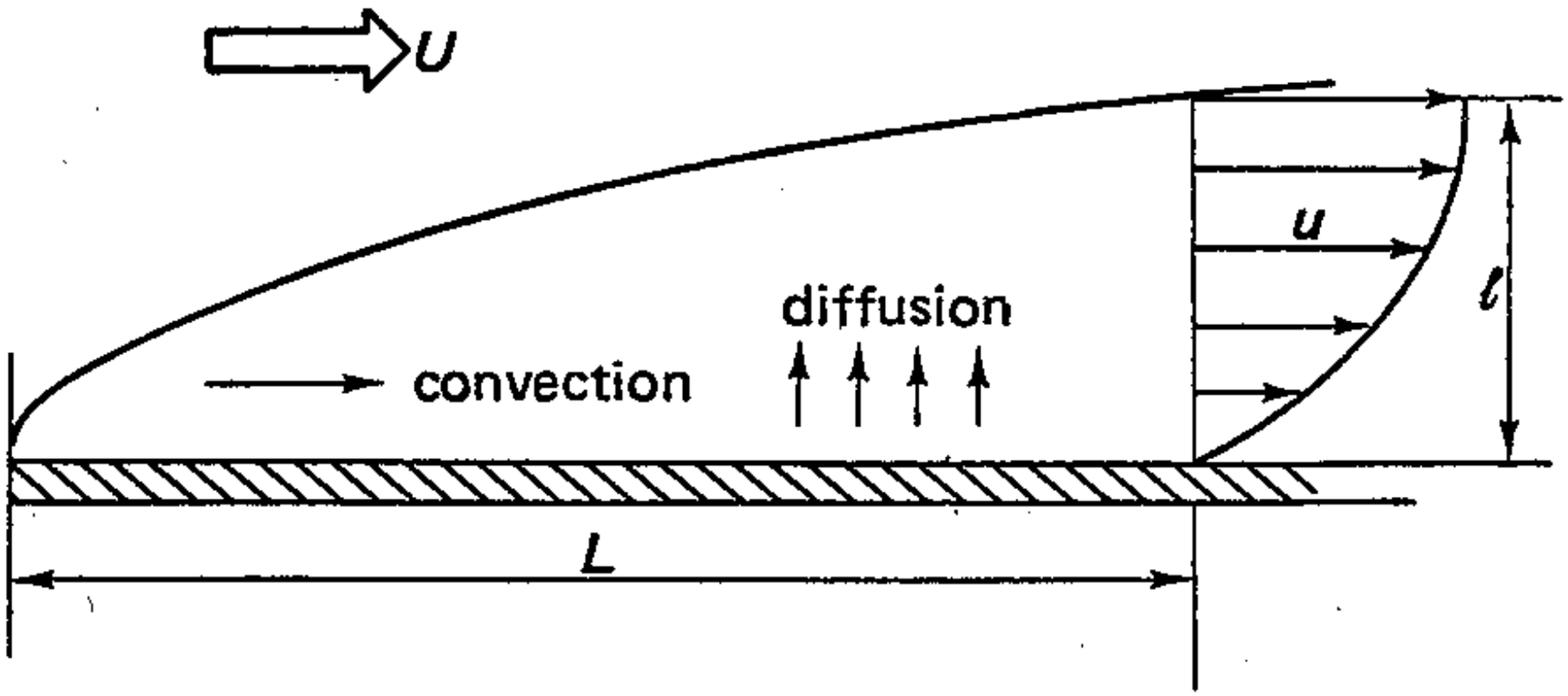

free troposphere

no-slip

Figure 1.2. Length scales, diffusion, and convection in a laminar boundary layer over a flat plate.

What is boundary layer depth l?

Steady Ekman BL equations (z = height, surface at $z = 0$, free troposphere is z) :

$$-fv = \nu\, d^2u/dz^2$$
$$f(u - G) = \nu\, d^2v/dz^2$$
$$u(0) = 0,\ u(\infty) = G$$
$$v(0) = 0,\ v(\infty) = 0$$

3-way balance of forces

no slip b.c. at z=0

Solution ($\zeta = z/\delta$) for BL velocity profile

$$u(z) = G(1 - e^{-\zeta} \cos \zeta)$$
$$v(z) = G\, e^{-\zeta} \sin \zeta$$

Flow adjusts to geostrophic within Ekman layer depth $\delta = (2\nu/f)^{1/2}$.
G is geostrophic velocity, ν is kinematic viscosity, f is Coriolis parameter.
For typical values of ν and f, $\delta = 1.7$ m!

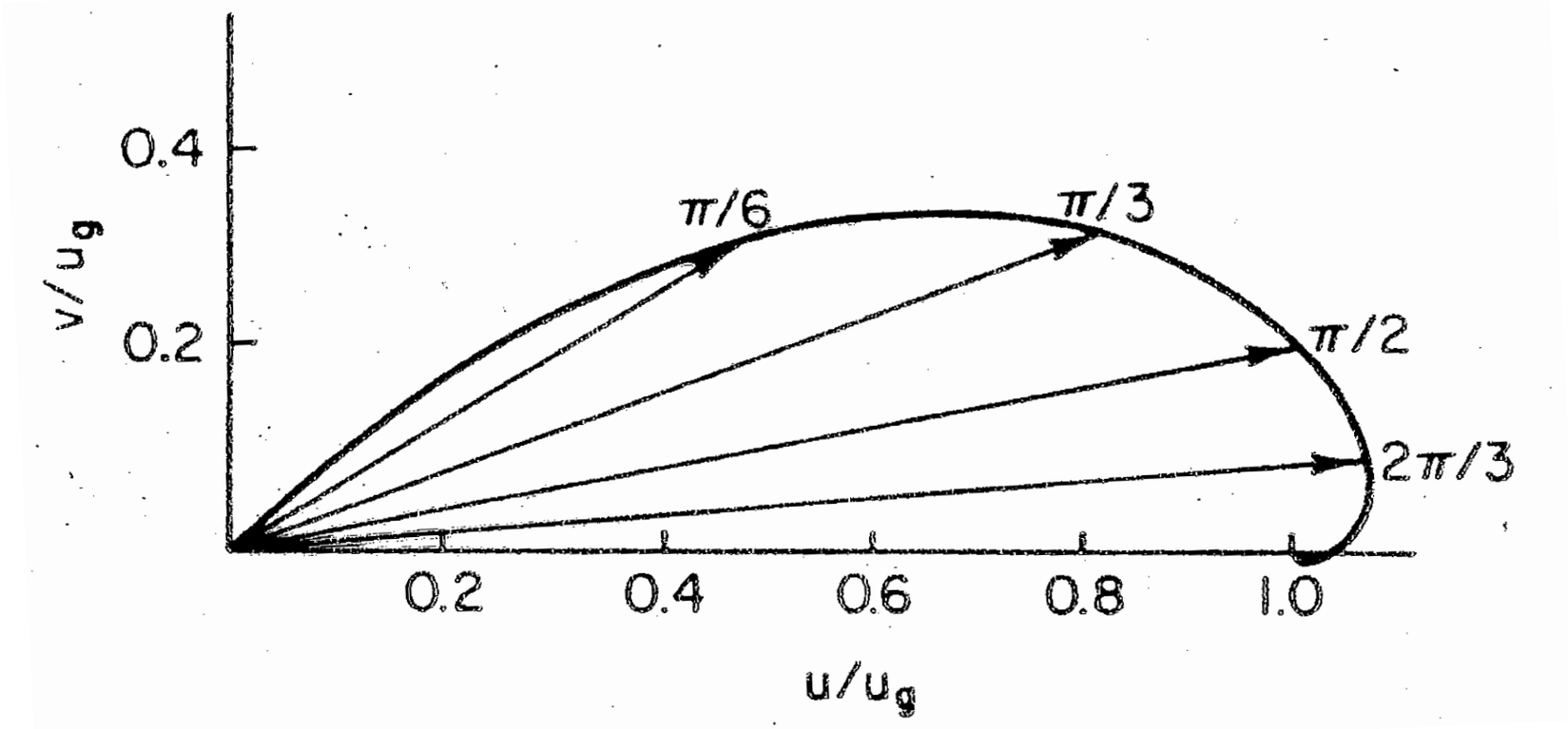

Turbulent Boundary Layer

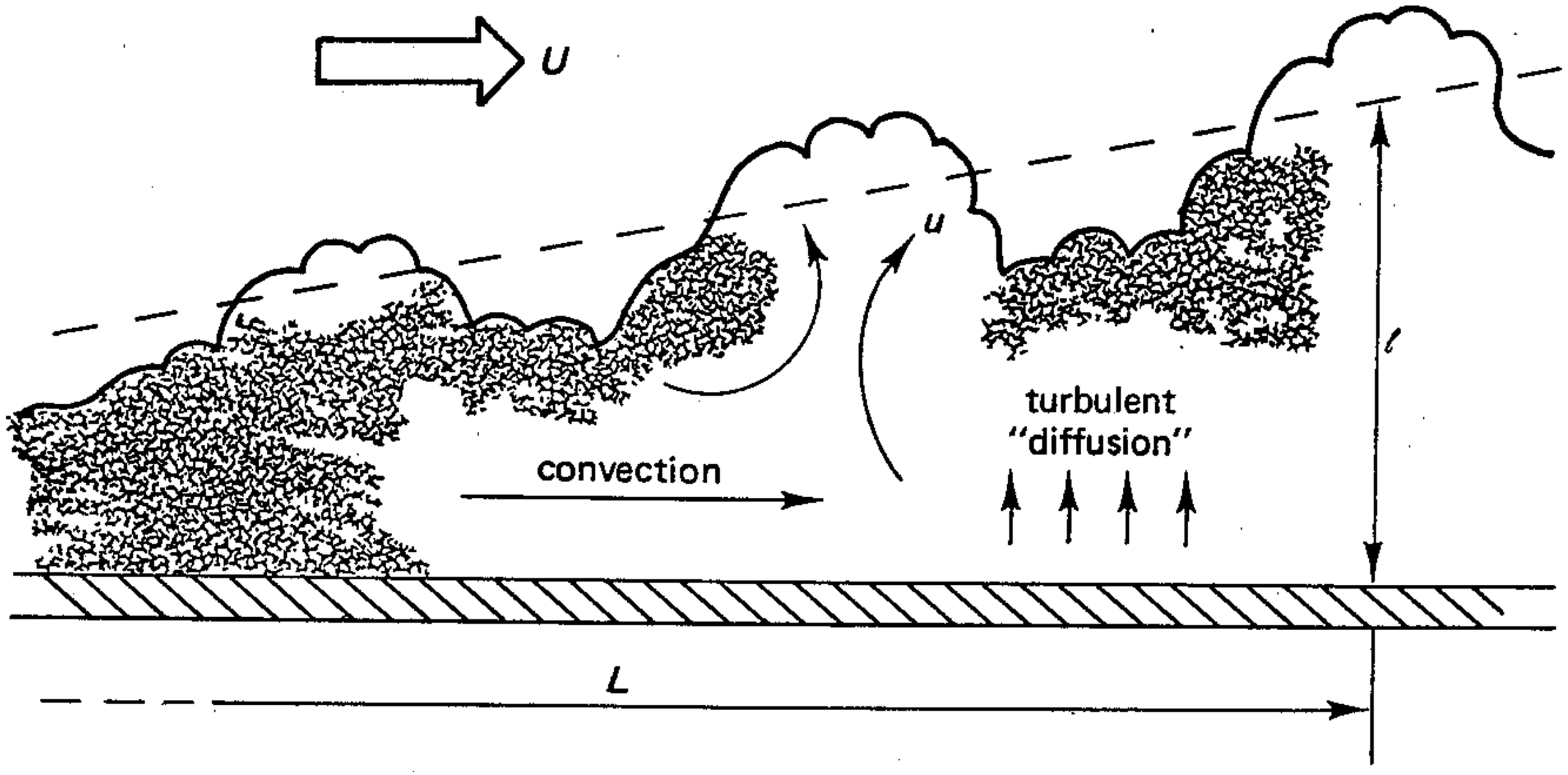

Figure 1.3. Length and velocity scales in a turbulent boundary layer. The time passed since the fluid at L passed the origin of the boundary layer is of order L/U.

What is boundary layer depth l?

Transition to turbulence in a boundary layer

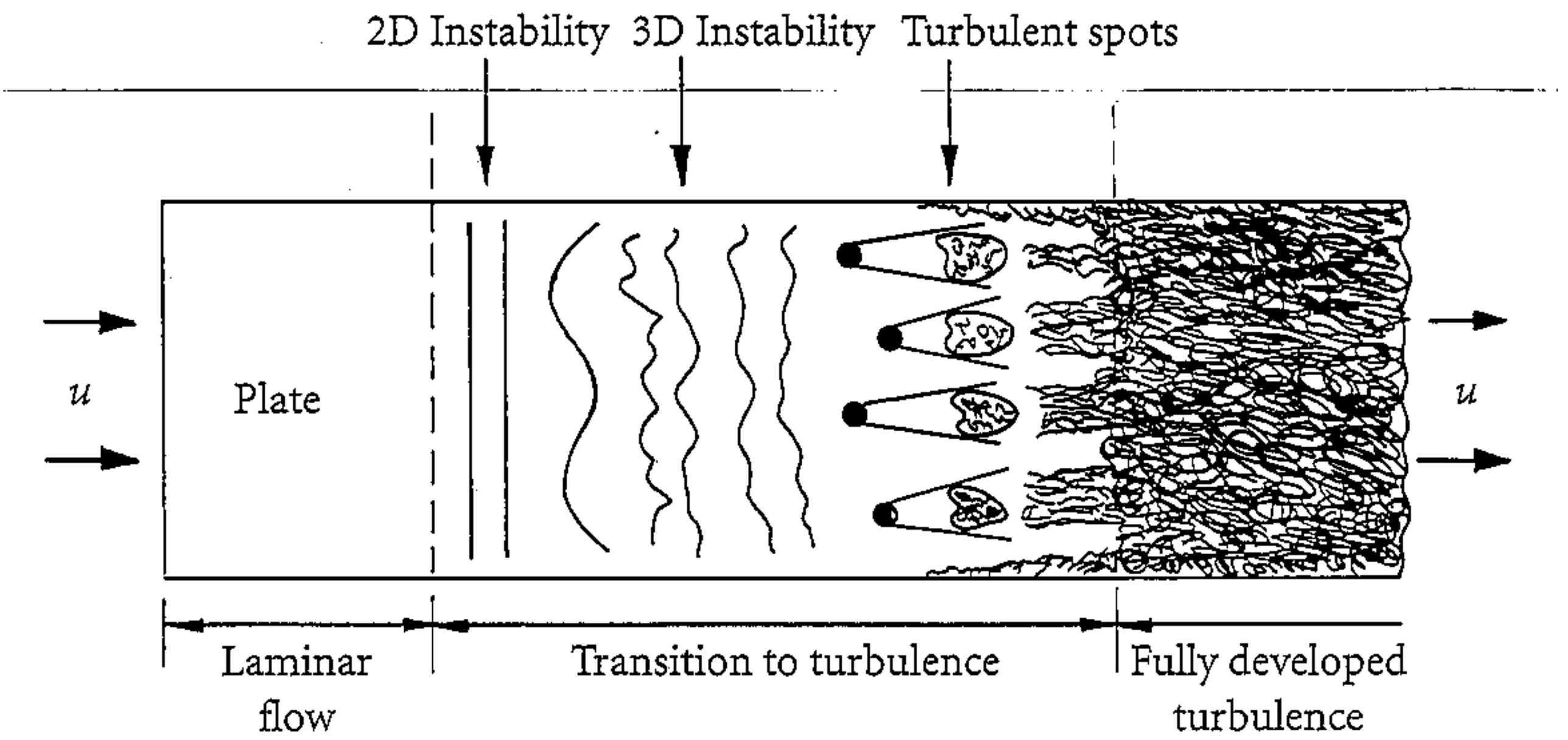

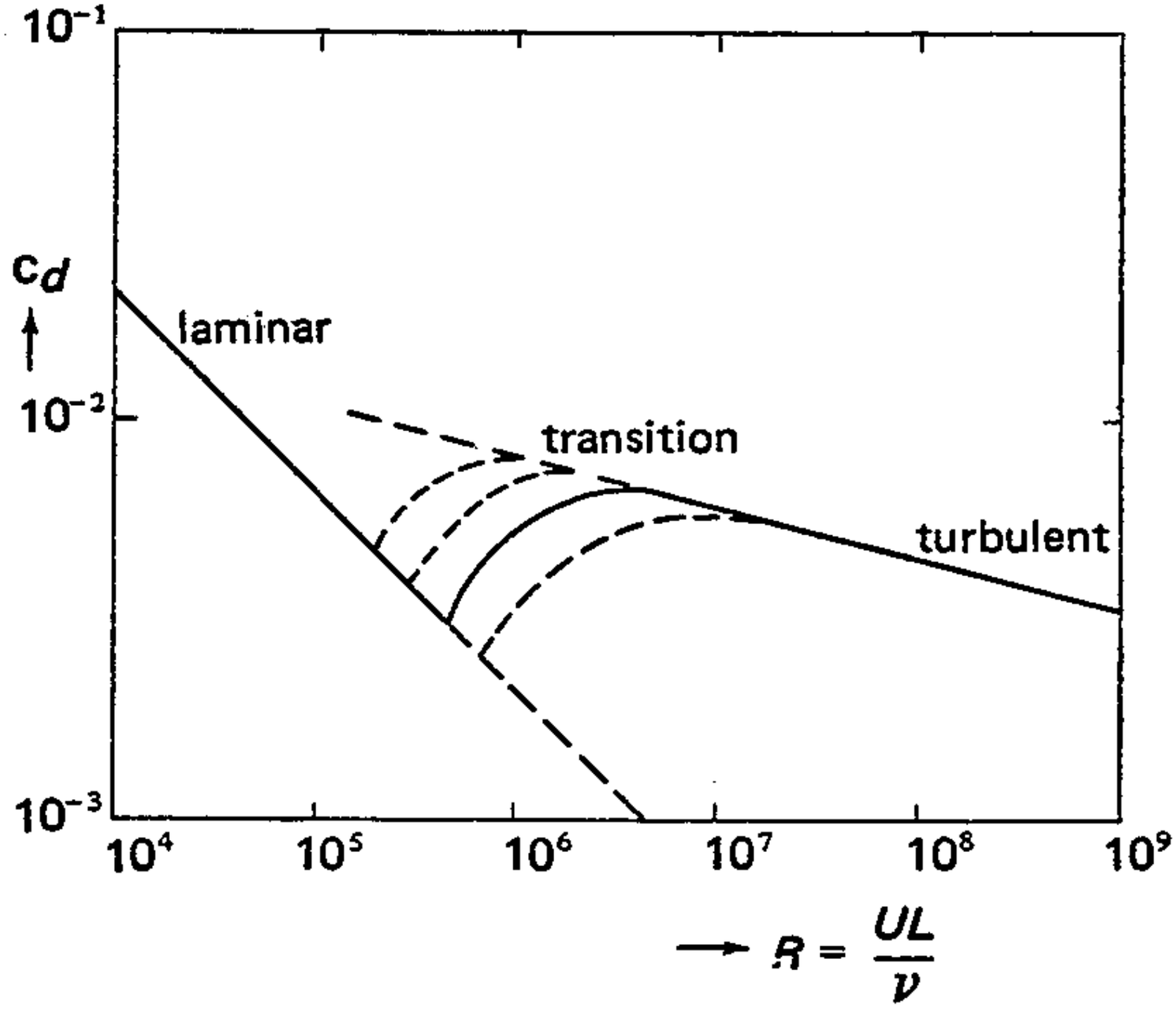

Drag is larger in turbulent flow.

Transition to turbulence is sensitive to small disturbances.

Figure 1.4. The drag coefficient of a flat plate. The several curves drawn in the transition range (partially laminar, partially turbulent flow over the plate) illustrate that transition is very sensitive to small disturbances.

Why is the boundary layer turbulent?

Hydrodynamic Instability

- An *instability* exists if a small disturbance grows in amplitude.
  - Shear Instabilities
    - Stratified Shear (Kelvin-Helmholtz) Instability
    - Convective (Rayleigh-Benard) Instability

Flow behind a cylinder at Re <1 to 10^6

For what Re does the flow become turbulent?

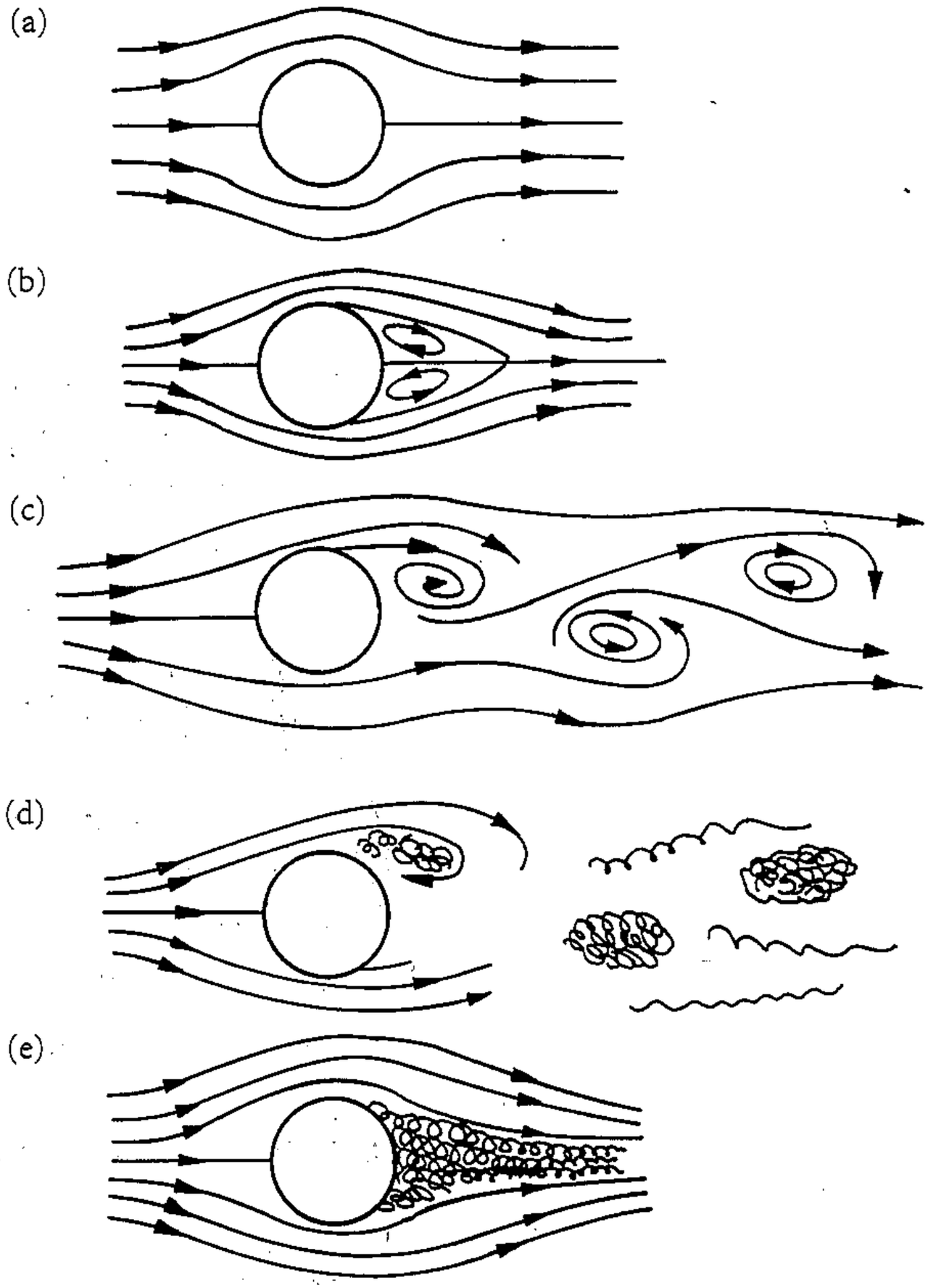

Figure 1.4 Flow behind a cylinder: (a) $Re < 1$; (b) $5 < Re < 40$; (c) $100 < Re < 200$; (d) $Re \sim 10^4$; and (e) $Re \sim 10^6$.

Flow Past a Cylinder

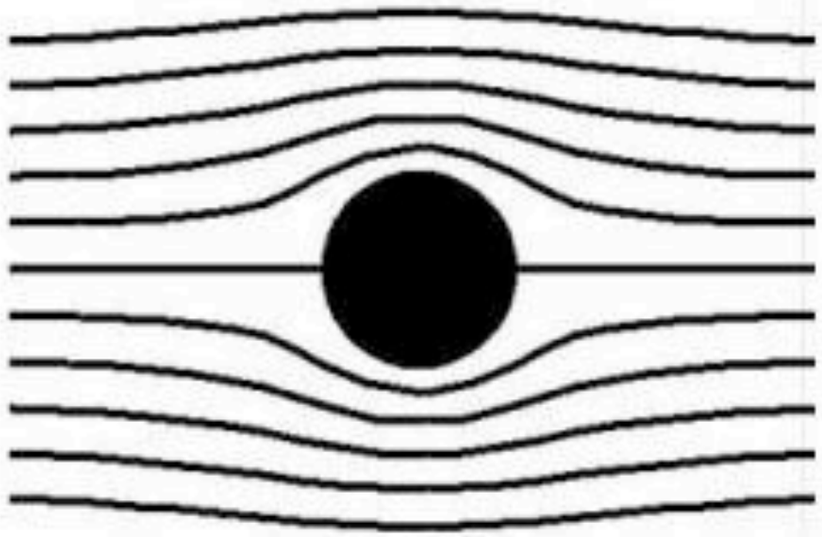

1. Ideal - Flow Attached

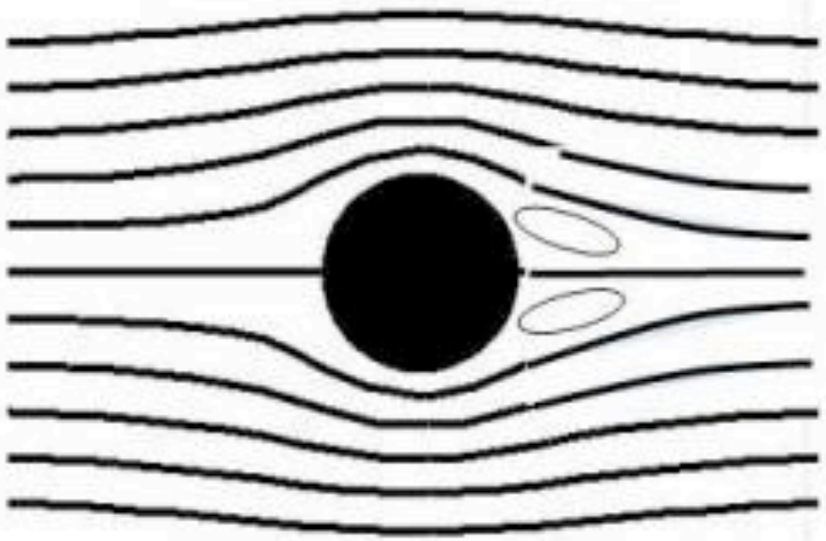

2. Separated - Steady

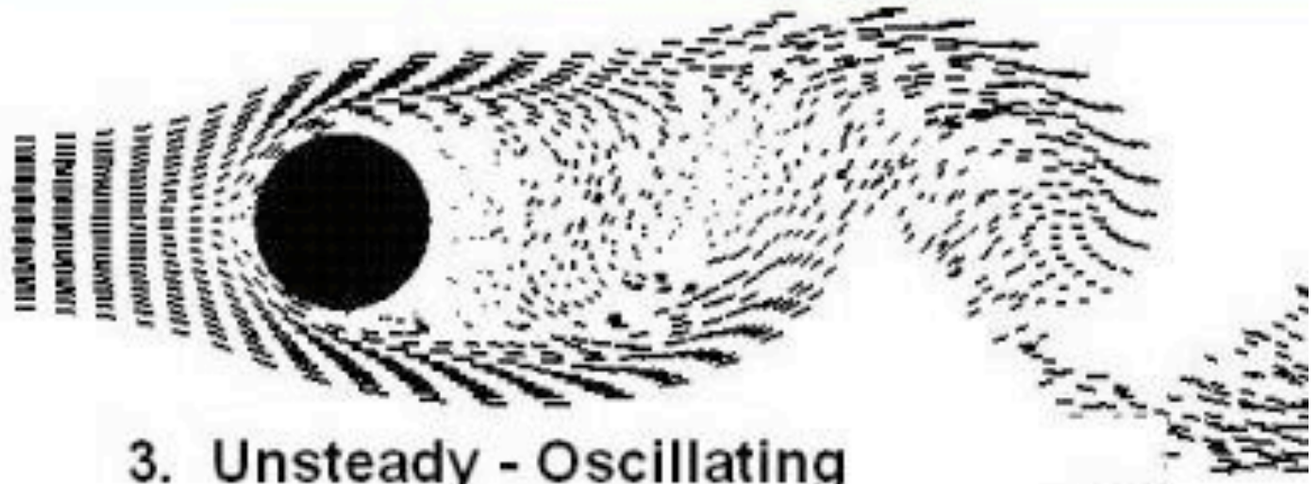

3. Unsteady - Oscillating

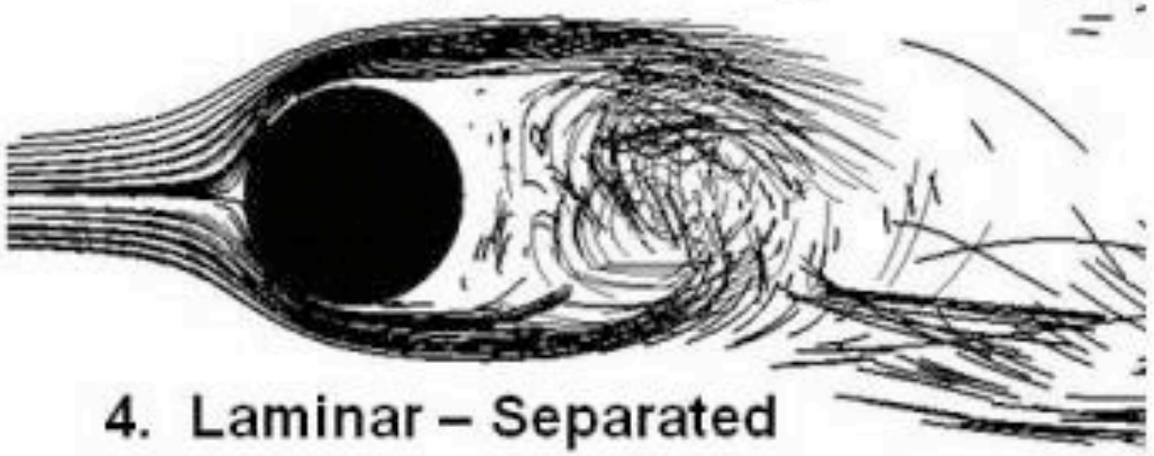

4. Laminar – Separated

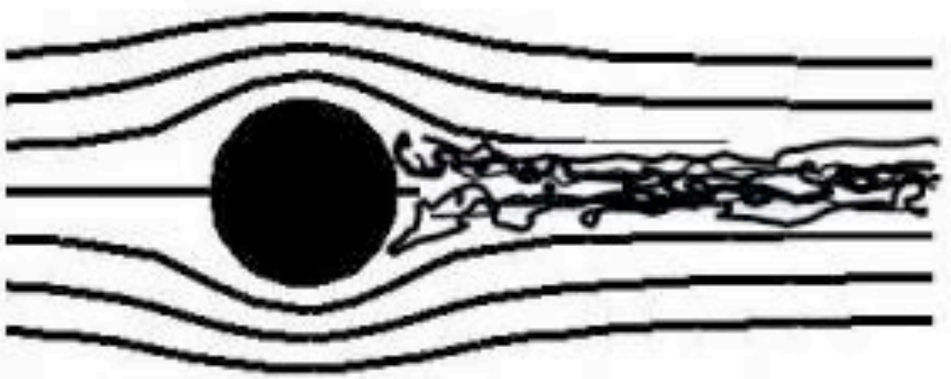

5. Turbulent – Separated

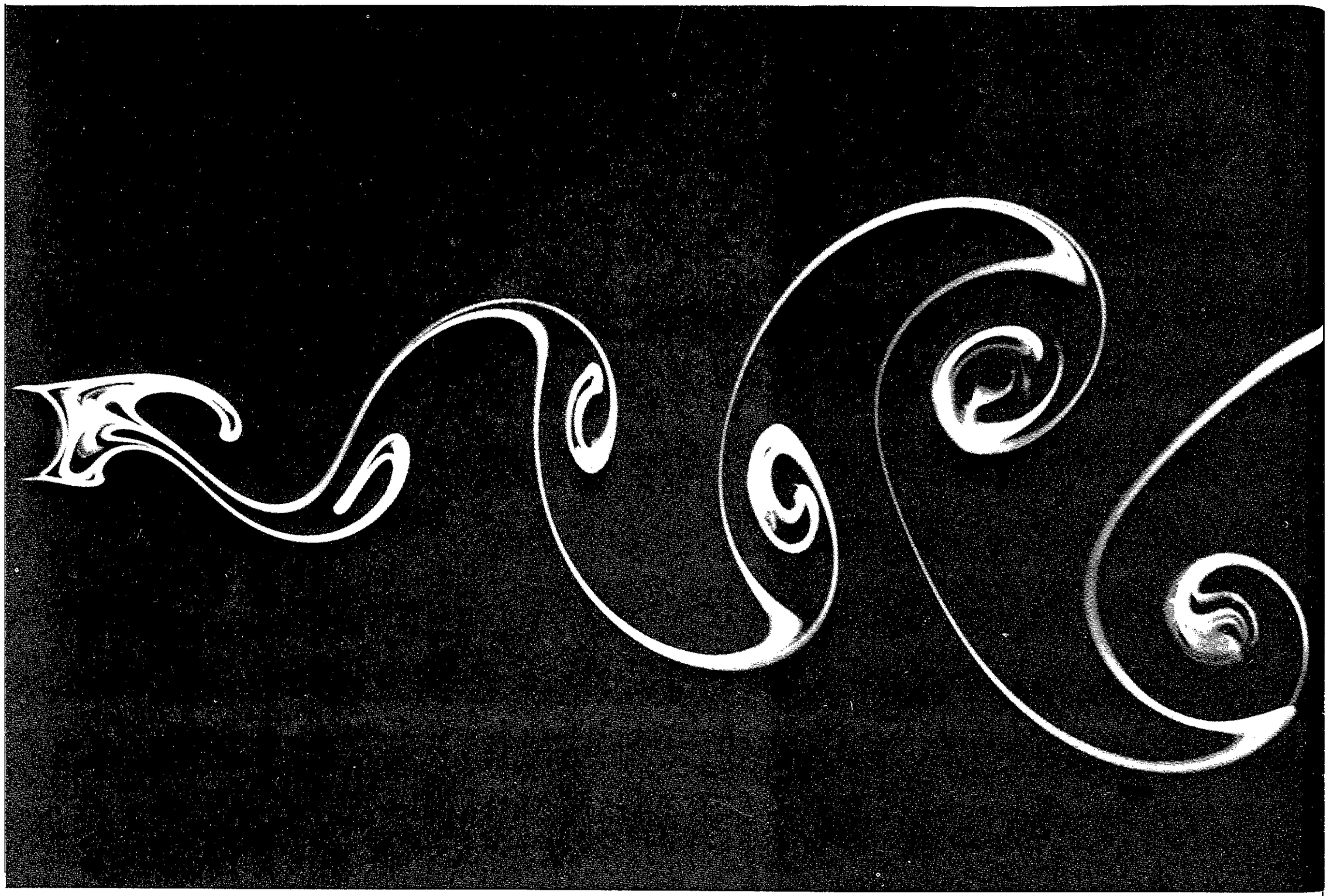

94. Kármán vortex street behind a circular cylinder at R=140. Water is flowing at 1.4 cm/s past a cylinder of diameter 1 cm. Integrated streaklines are shown by electrolytic precipitation of a white colloidal smoke, illuminated by a sheet of light. The vortex sheet is seen to grow in width downstream for some diameters. *Photograph by Sadatoshi Taneda*

Vortex instability: another transition to turbulence

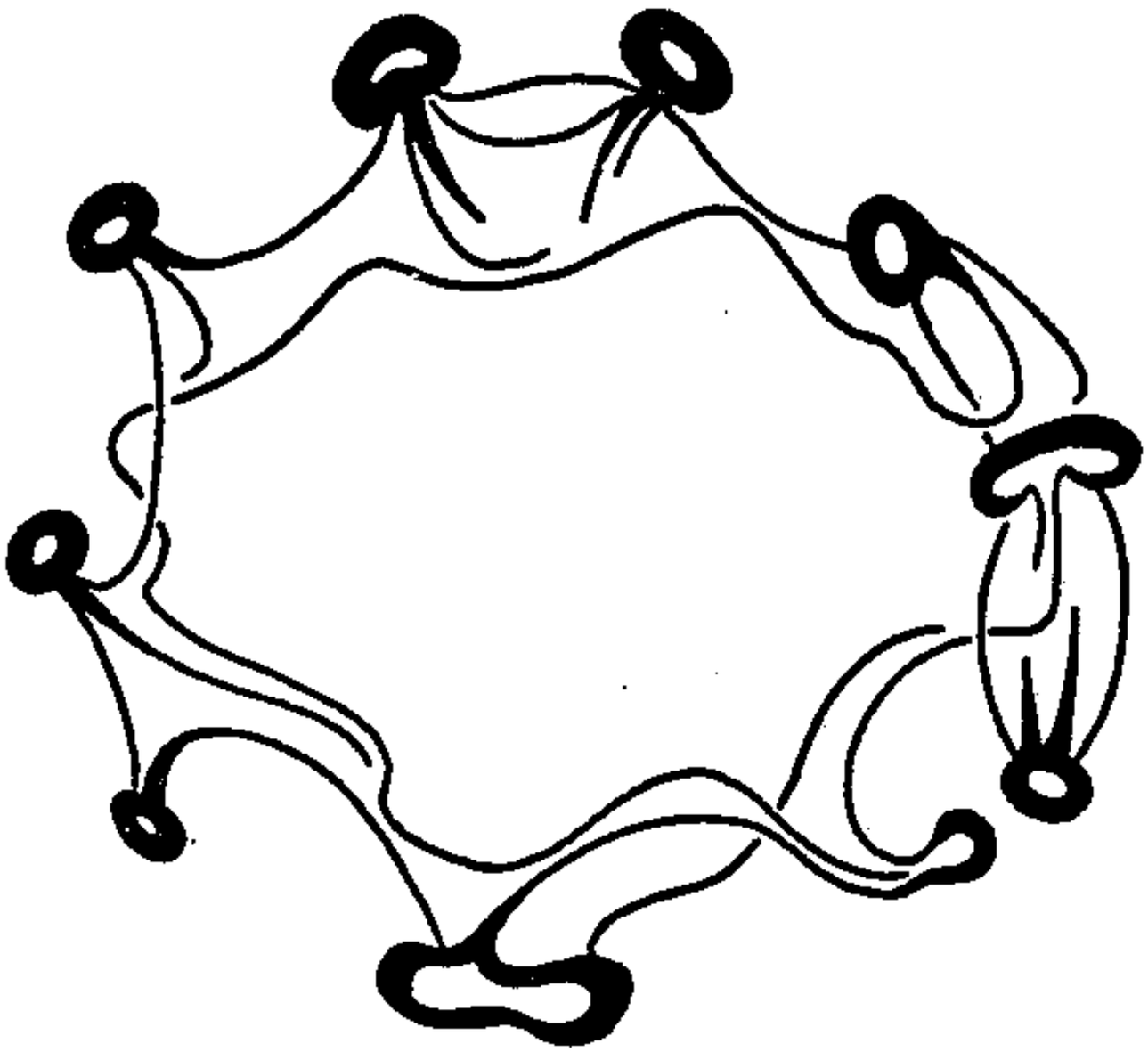

Figure 1.5. Sketch of the nonlinear breakdown of a drop of ink in water.

Instability of a Laminar Vortex Ring

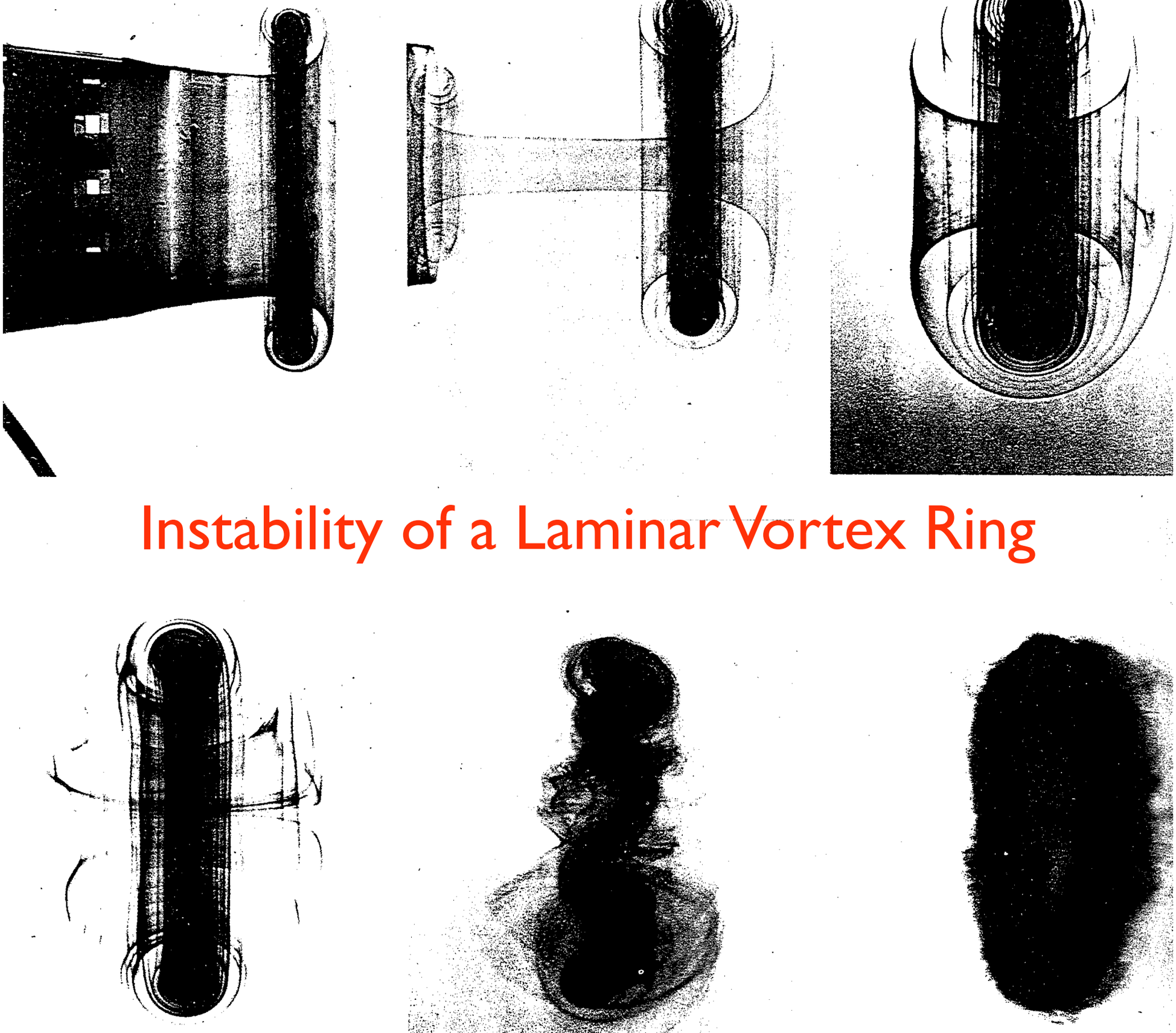

Instability of a pair of trailing vortices

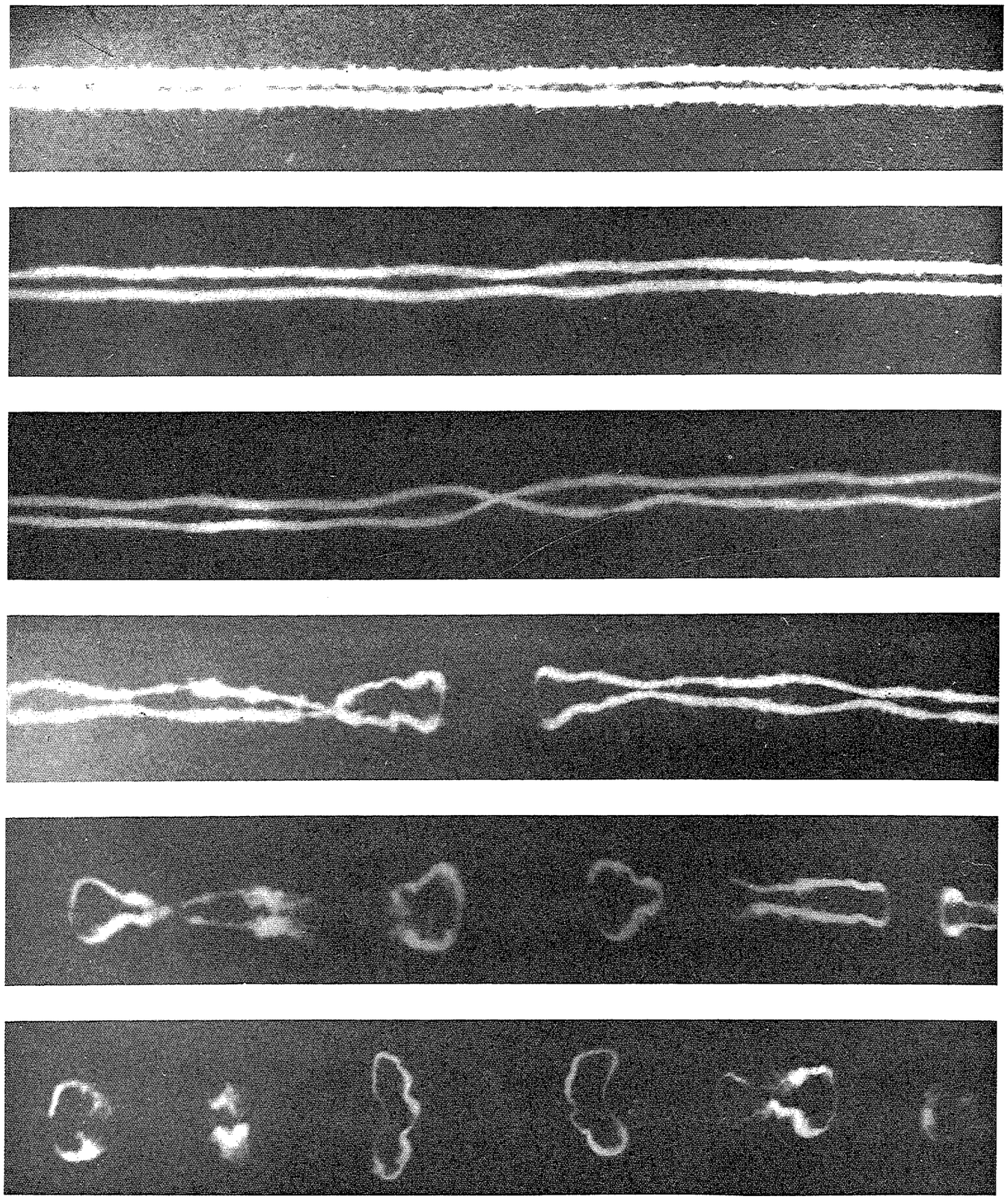

116. Instability of a pair of trailing vortices. The vortex trail of a B-47 aircraft was photographed directly overhead at intervals of 15 s after its passage. The vortex cores are made visible by condensation of moisture. They slowly recede and draw together in a symmetrical nearly sinusoidal pattern until they connect to form a train of vortex rings. The wake then quickly disintegrates. This is commonly called Crow instability after the researcher who explained its early stages analytically. *Crow 1970, courtesy of Meteorology Research Inc.*

Instability of an Axisymmetric Jet

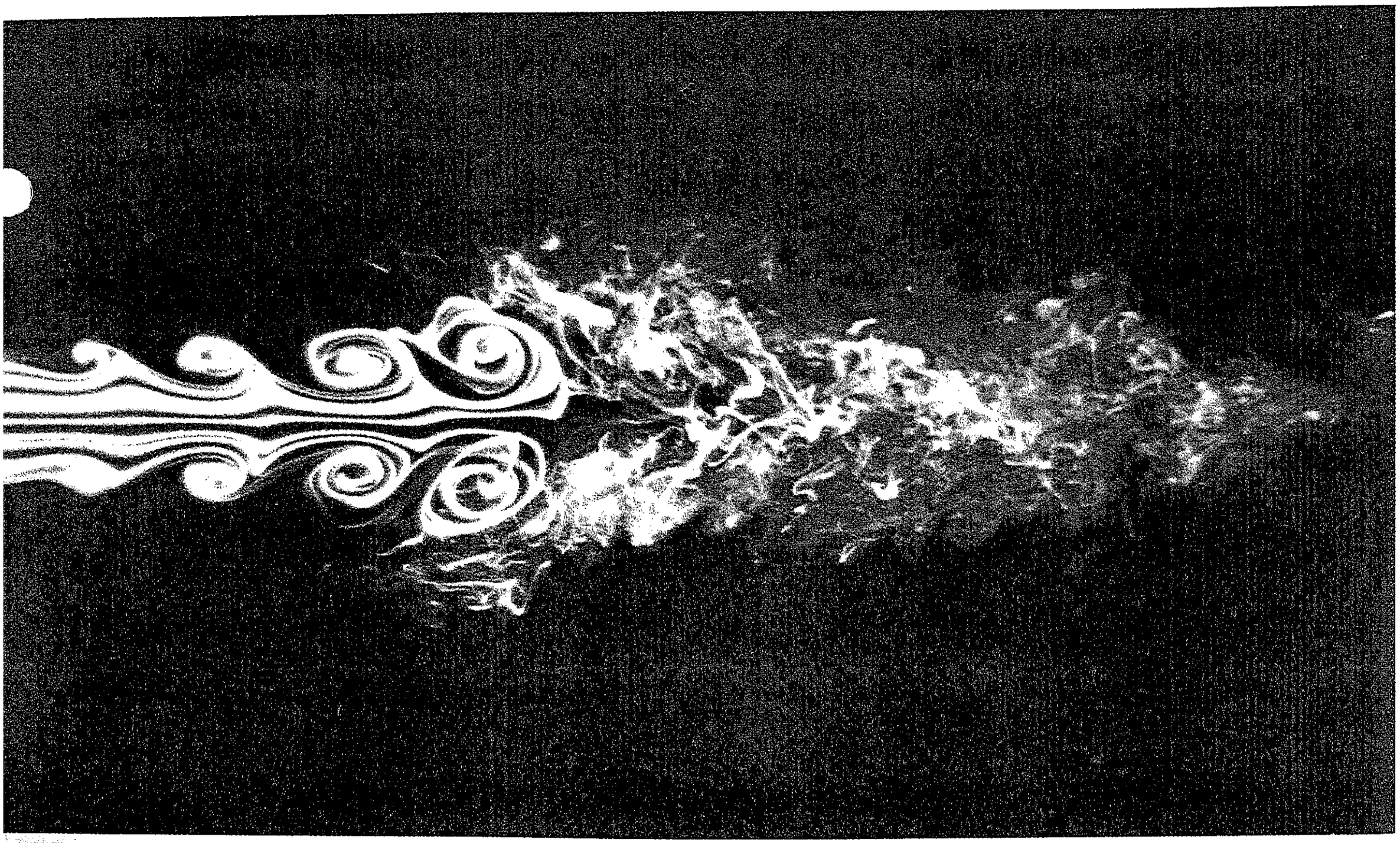

102. Instability of an axisymmetric jet. A laminar stream of air flows from a circular tube at Reynolds number 10,000 and is made visible by a smoke wire. The edge of the jet develops axisymmetric oscillations, rolls up into vortex rings, and then abruptly becomes turbulent. *Photograph by Robert Drubka and Hassan Nagib*

Turbulent water jet

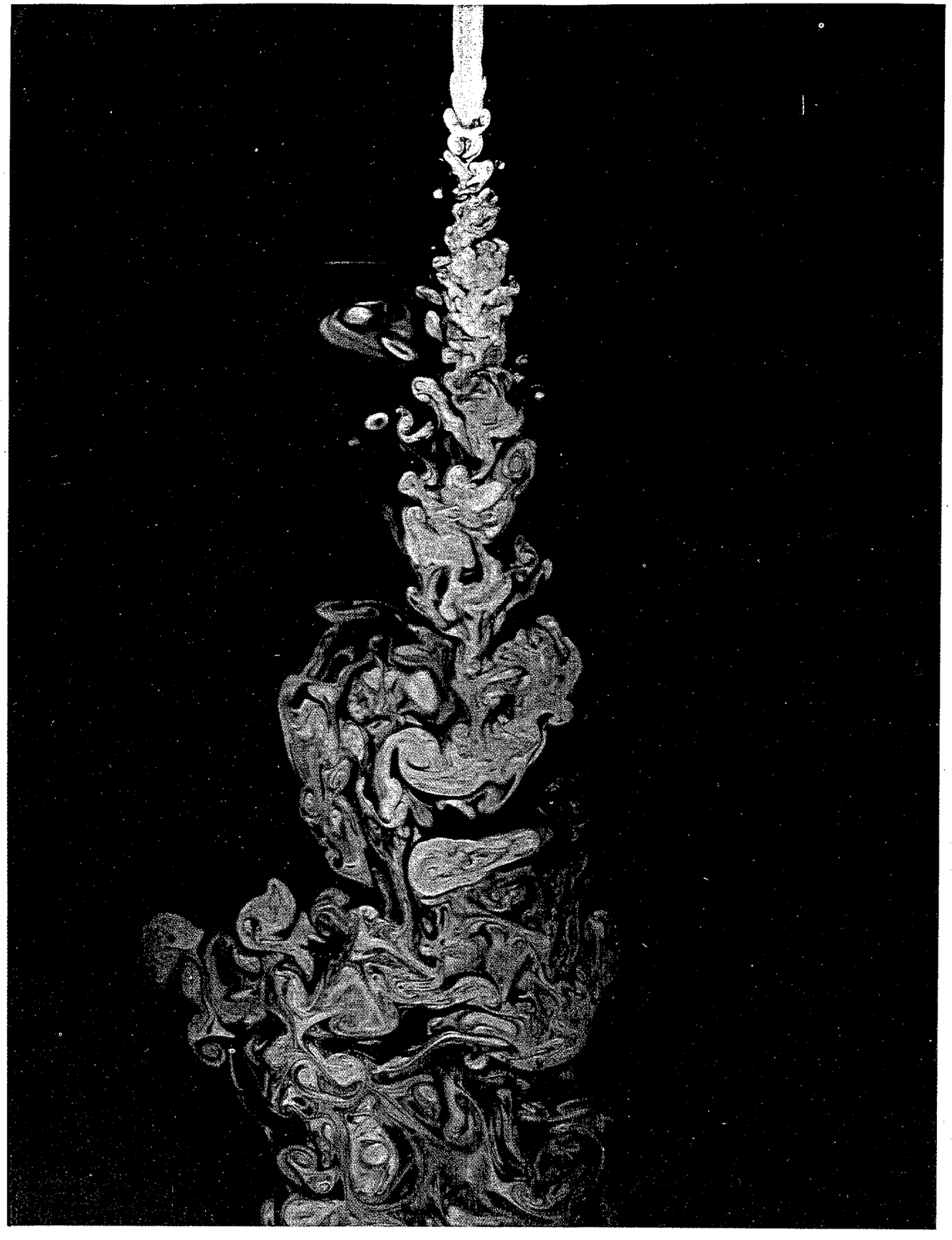

166. Turbulent water jet. Laser-induced fluorescence shows the concentration of jet fluid in the plane of symmetry of an axisymmetric jet of water directed downward into water. The Reynolds number is approximately 2300. The spatial resolution is adequate to resolve the Kolmogorov scale in the downstream half of the photograph. *Dimotakis, Lye & Papantoniou 1981*

Kelvin-Helmholtz instability of stratified shear flow

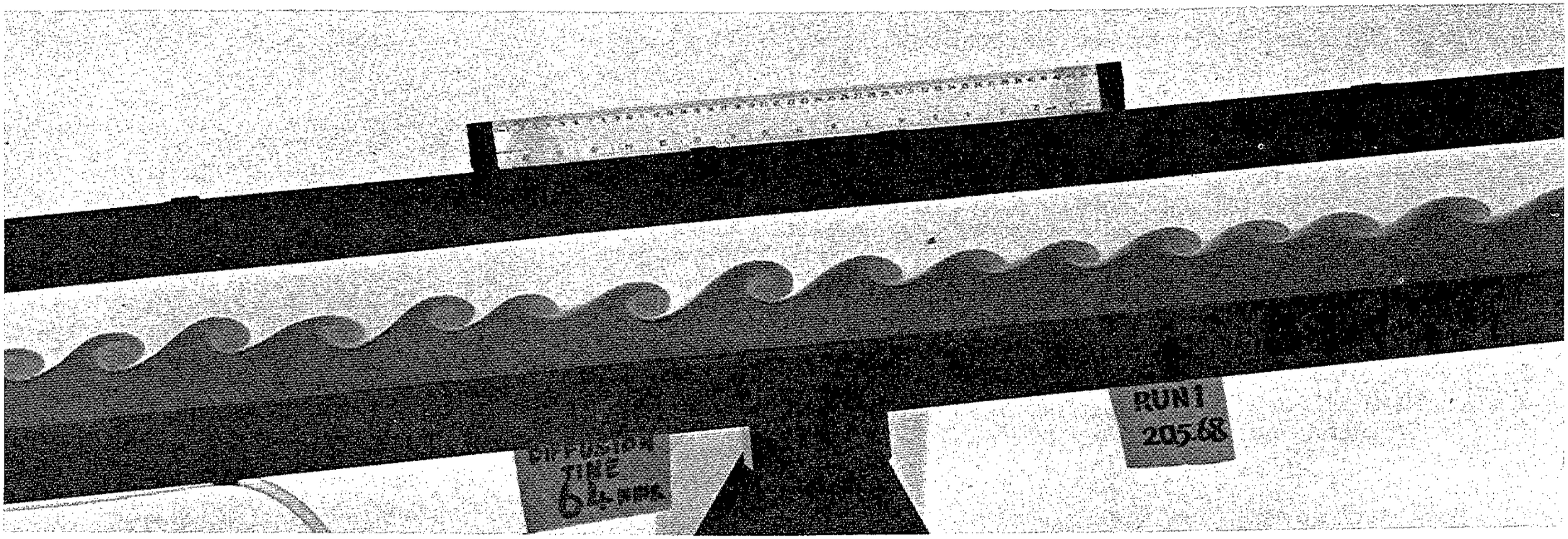

145. Kelvin-Helmholtz instability of stratified shear flow. A long rectangular tube, initially horizontal, is filled with water above colored brine. The fluids are allowed to diffuse for about an hour, and the tube then quickly tilted six degrees, setting the fluids into motion. The brine accelerates uniformly down the slope, while the water above similarly accelerates up the slope. Sinusoidal instability of the interface occurs after a few seconds, and has here grown nonlinearly into regular spiral rolls. *Thorpe 1971*

Kelvin-Helmholtz instability

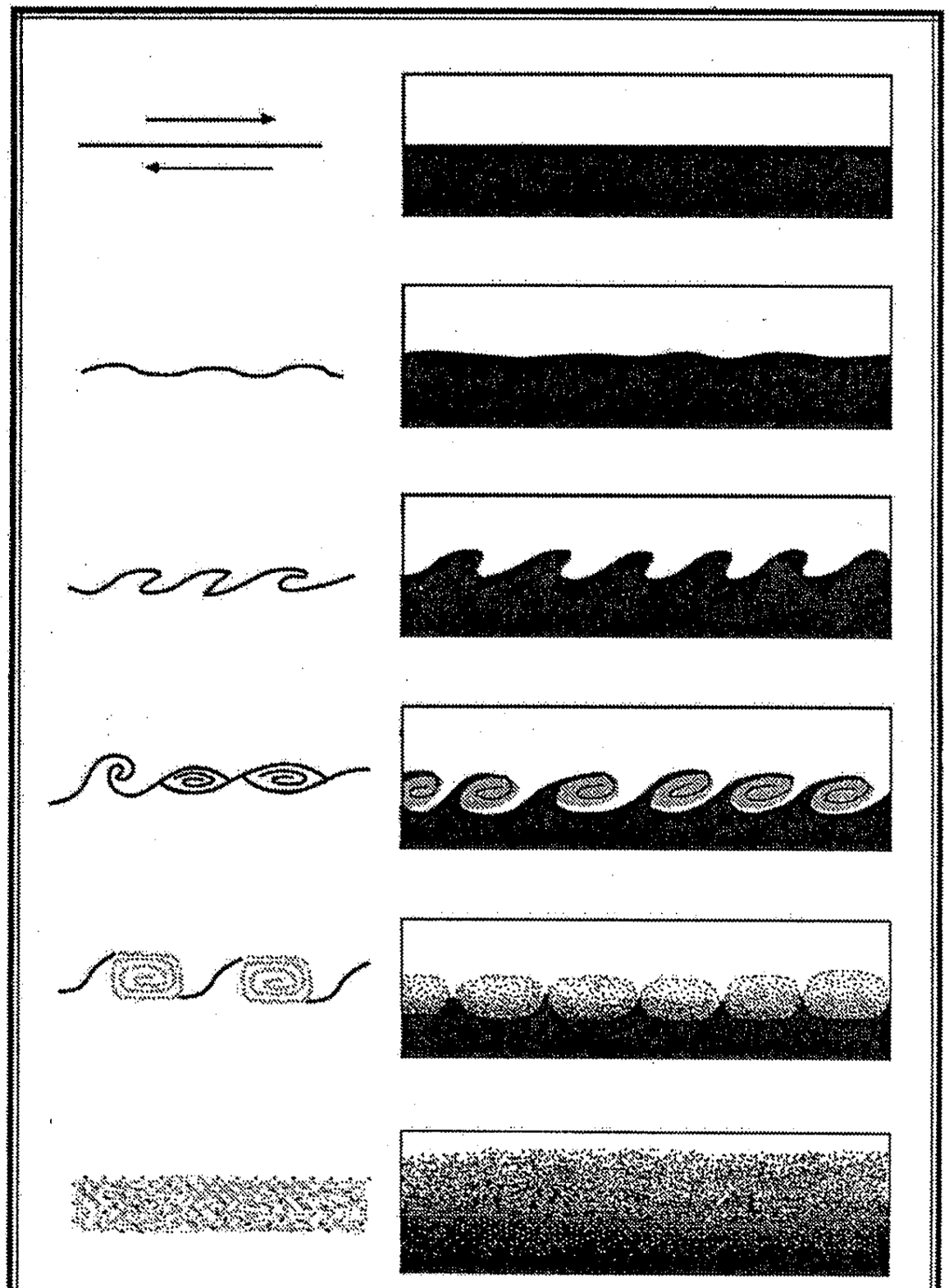

Fig. 5.18 Schematic diagram of Kelvin-Helmholtz instability in a laboratory experiment where shear flow has been generated. The upper layer, water, flows to the right, and the lower more dense fluid, dyed brine, flows to the left. The figures are about half a second apart. After Thorpe (1969,1973) and Woods (1969).

2D numerical simulation of Kelvin-Helmholtz instability

Stability parameter relationships

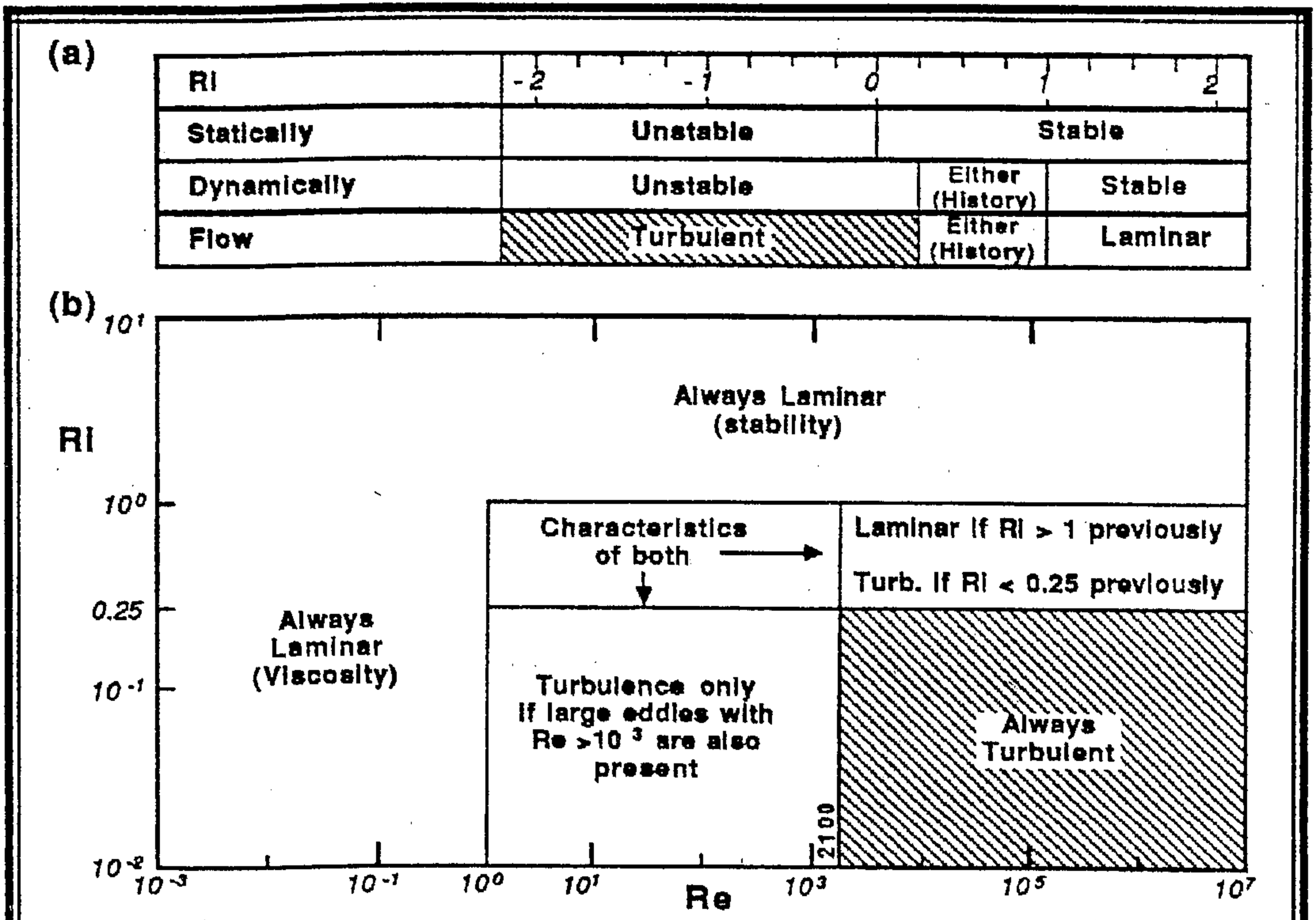

Fig. 5.24 Stability parameter relationships (see text). (After Woods, 1969).

Global convective instability

Figure 1.3 Fluid is held between two flat, parallel plates. The lower plate is heated. At low values of ΔT the fluid is quiescent. As ΔT is increased natural convection sets in, first in the form of regular convection cells and then in the form of turbulent flow.

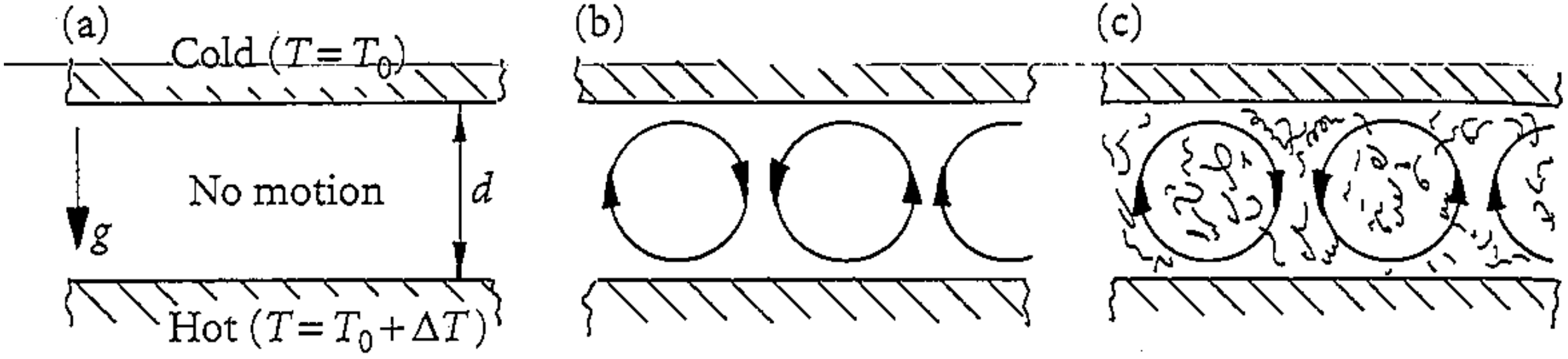

Buoyancy-driven convection rolls

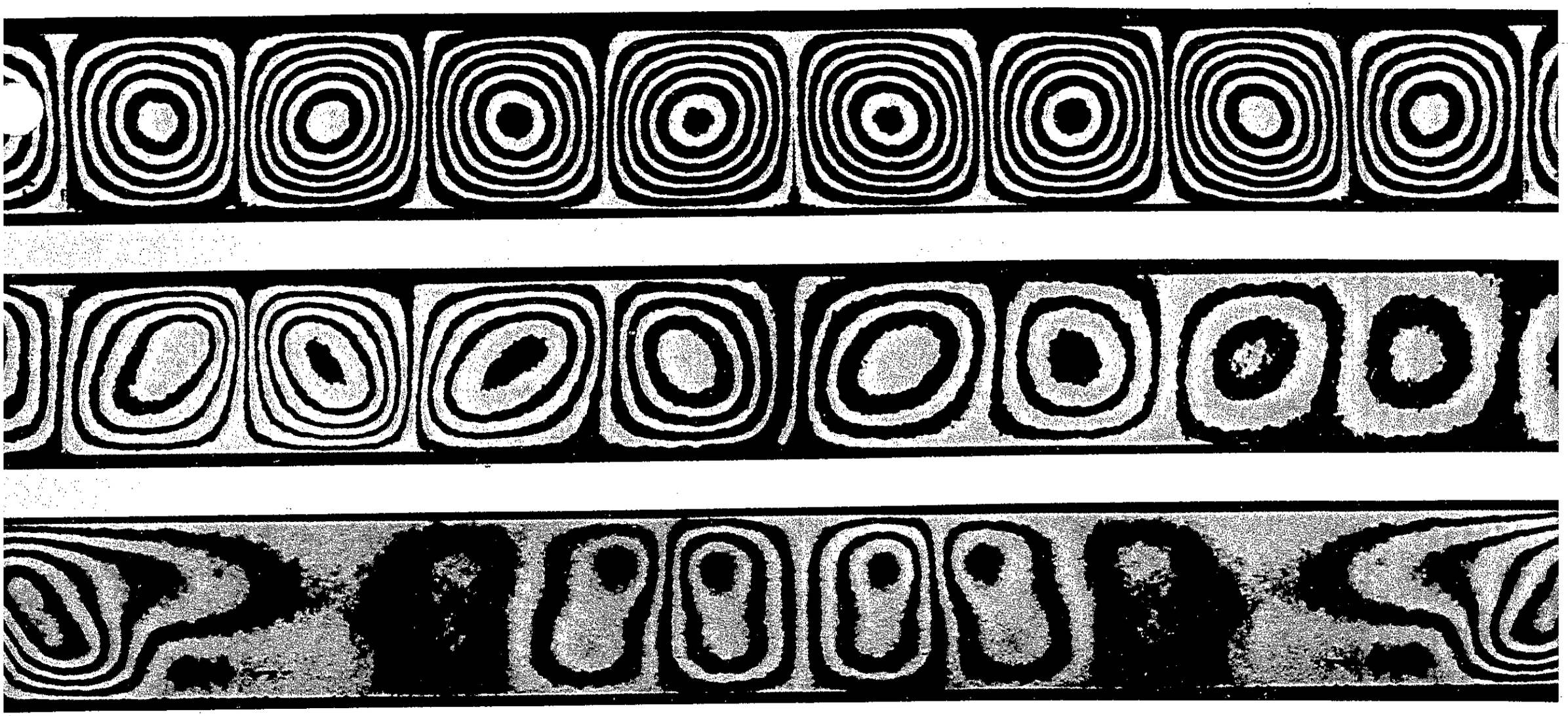

139. Buoyancy-driven convection rolls. Differential interferograms show side views of convective instability of silicone oil in a rectangular box of relative dimensions 10:4:1 heated from below. At the top is the classical Rayleigh-Bénard situation: uniform heating produces rolls parallel to the shorter side. In the middle photograph the temperature difference and hence the amplitude of motion increase from right to left. At the bottom, the box is rotating about a vertical axis. *Oertel & Kirchartz 1979, Oertel 1982a*

Buoyancy-driven convection rolls

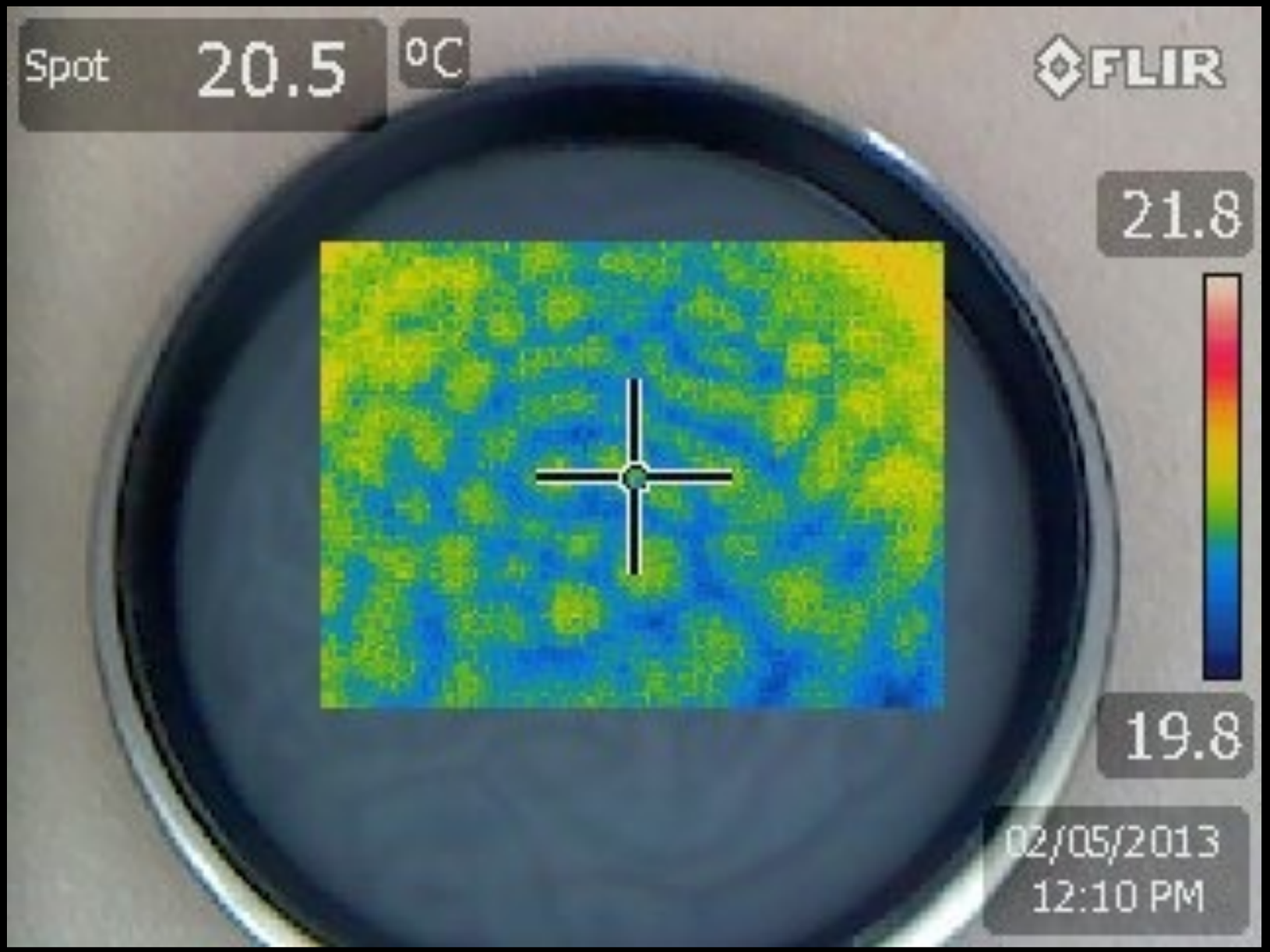

Buoyancy-driven convection rolls

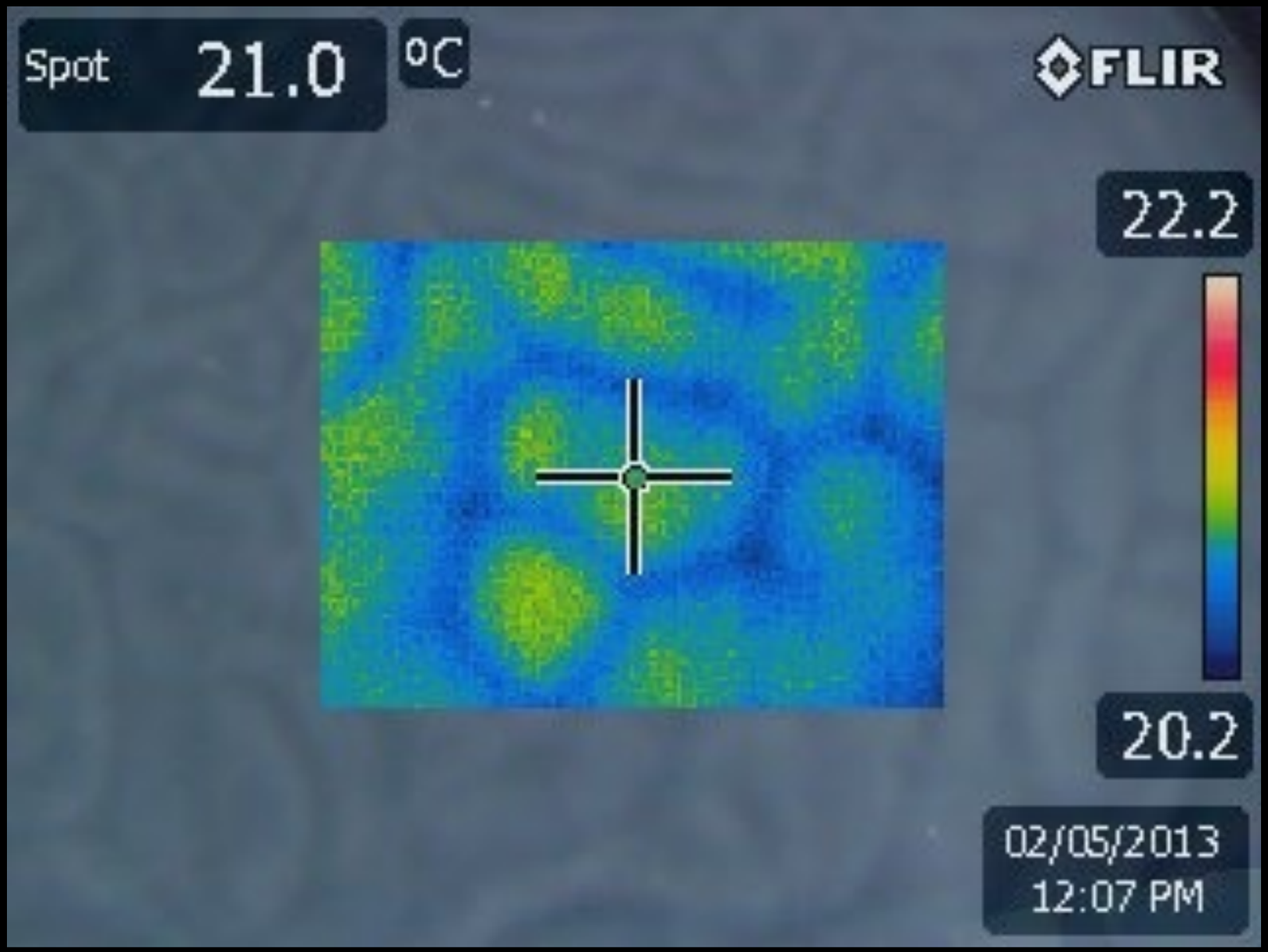

Boundary layer cloud 'streets'

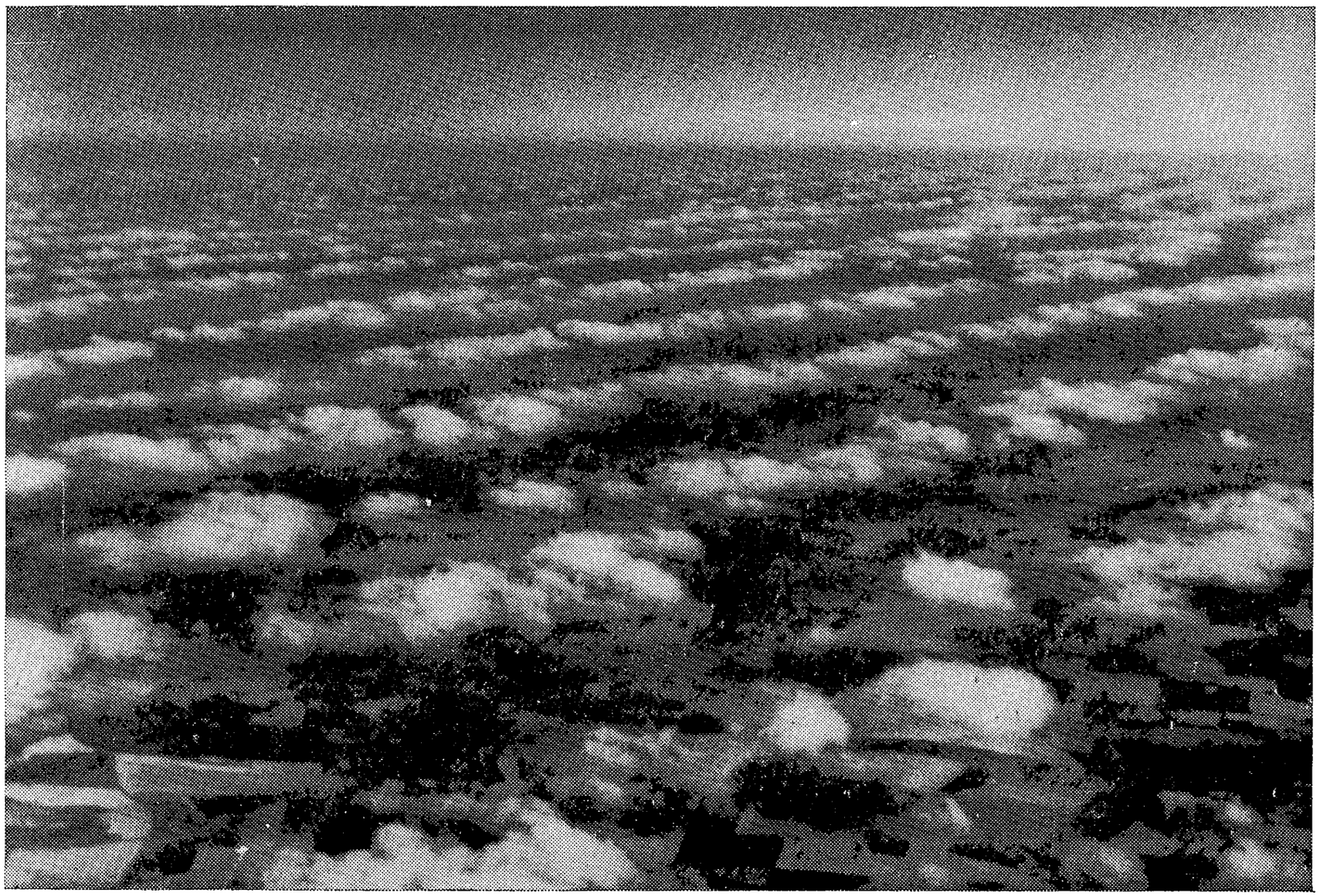

Fig. 7.2. Convective clouds in an unstable layer, aligned in 'streets' along the direction of shear. (Compare with fig. 4.14 pl. x, which shows clouds formed by a shear instability and aligned across the flow. The form of 'billow' clouds can vary widely according to the relative importance of shear and convection.) (Photograph: R. S. Scorer.)

Turbulence is random and unpredictable

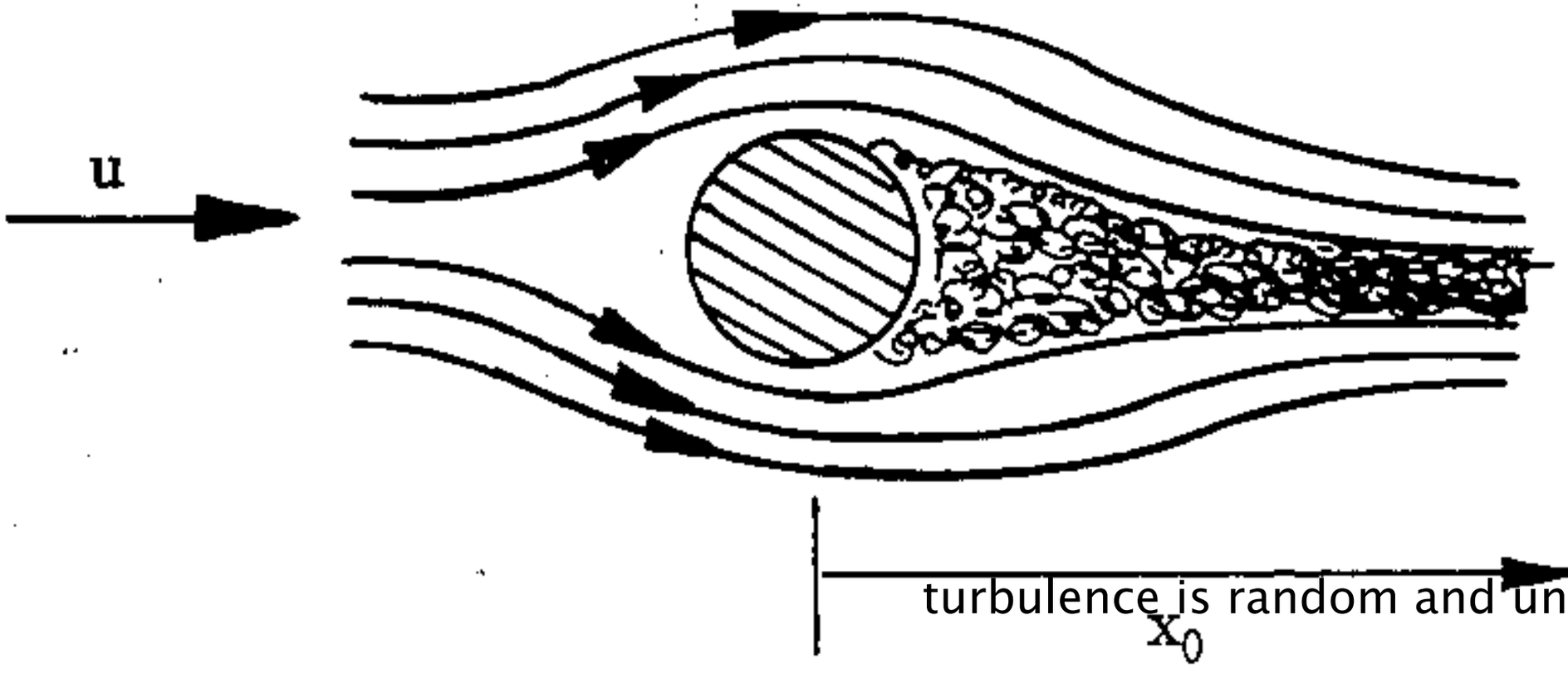

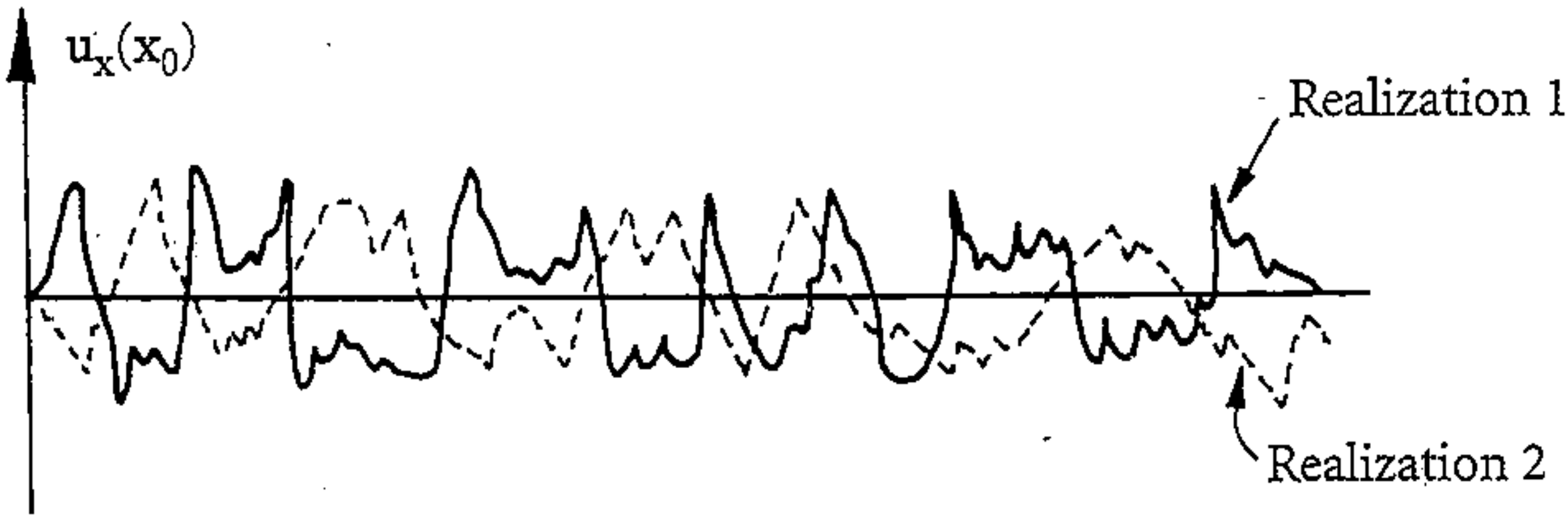

Range of spatial scales increases with Re

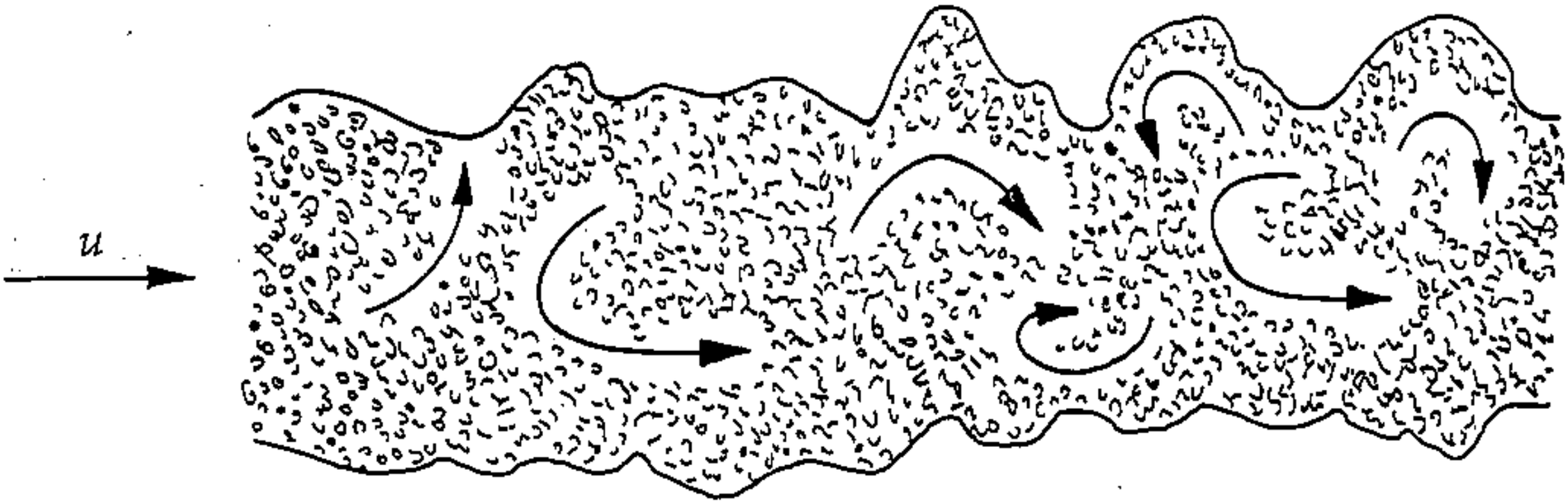

High Re

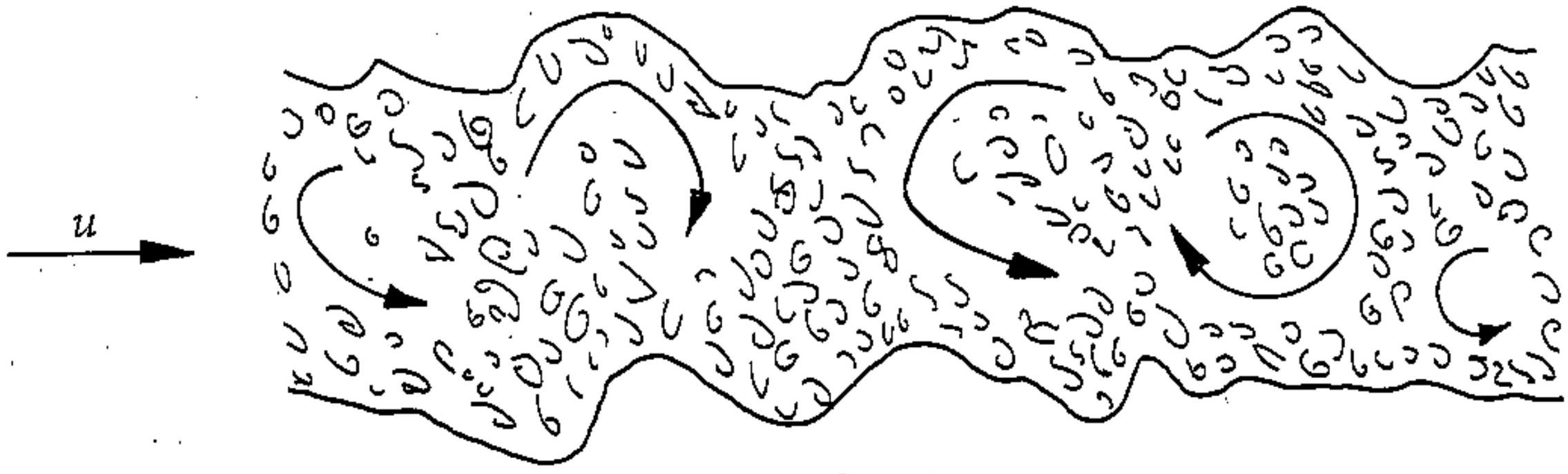

Modest Re

Energy cascade

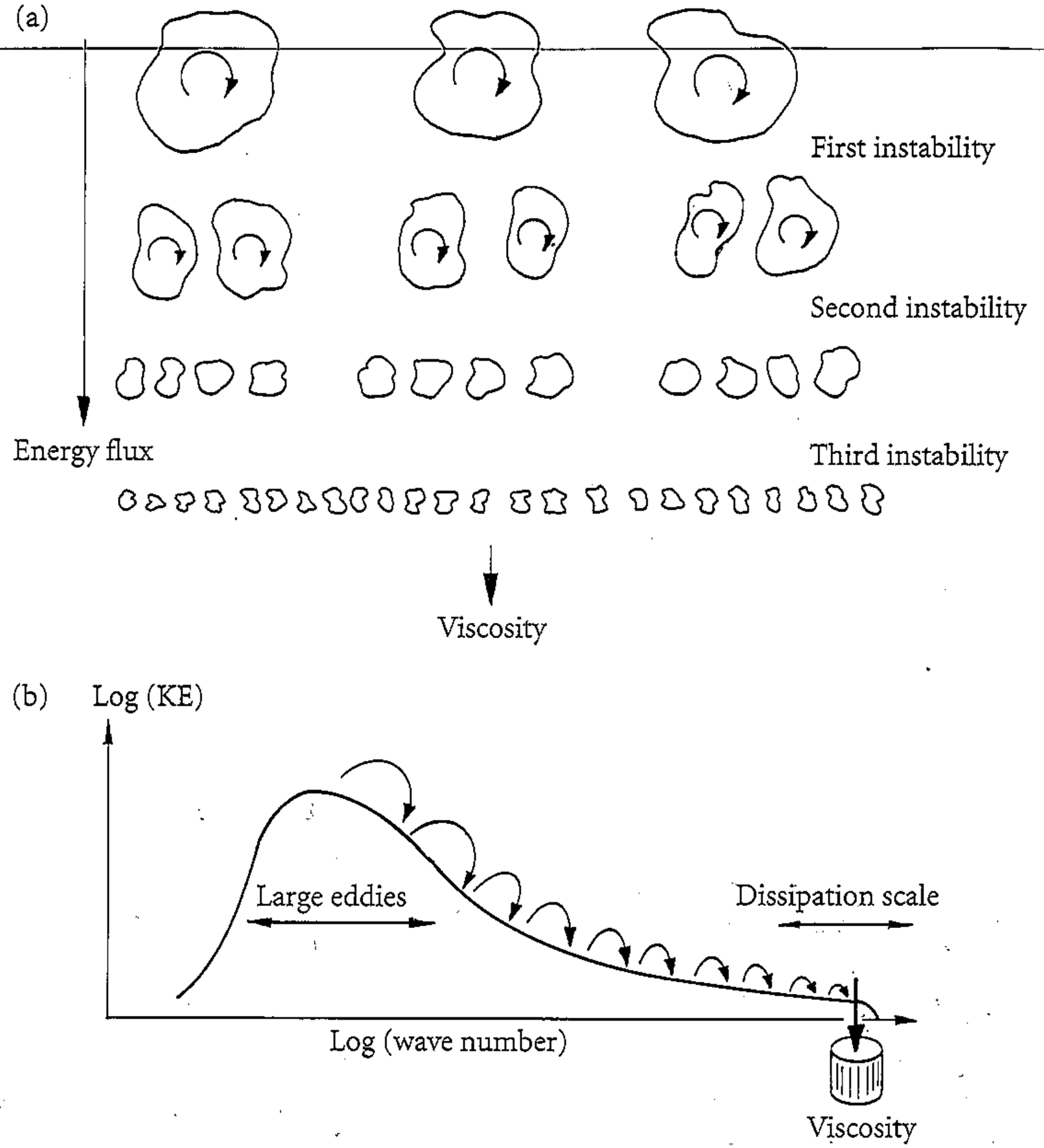

Figure 3.9 (a) A schematic representation of the energy cascade (after Frisch). (b) The energy cascade in terms of energy versus wave number.